



HAL
open science

First detection of fluorine on Mars: Implications for Gale Crater's geochemistry

Olivier Forni, Michael Gaft, Michael Toplis, Samuel Clegg, Sylvestre Maurice,
Roger Wiens, Nicolas Mangold, Olivier Gasnault, Violaine Sautter, Stéphane
Le Mouélic, et al.

► To cite this version:

Olivier Forni, Michael Gaft, Michael Toplis, Samuel Clegg, Sylvestre Maurice, et al.. First detection of fluorine on Mars: Implications for Gale Crater's geochemistry. *Geophysical Research Letters*, 2015, 42 (4), pp.1020-1028. 10.1002/2014GL062742 . hal-02373397

HAL Id: hal-02373397

<https://hal.science/hal-02373397>

Submitted on 8 Jul 2021

HAL is a multi-disciplinary open access archive for the deposit and dissemination of scientific research documents, whether they are published or not. The documents may come from teaching and research institutions in France or abroad, or from public or private research centers.

L'archive ouverte pluridisciplinaire **HAL**, est destinée au dépôt et à la diffusion de documents scientifiques de niveau recherche, publiés ou non, émanant des établissements d'enseignement et de recherche français ou étrangers, des laboratoires publics ou privés.

Copyright



RESEARCH LETTER

10.1002/2014GL062742

Key Points:

- First detection of fluorine at the Martian surface
- High sensitivity of fluorine detection with LIBS
- F-bearing phases imply alteration and evolved magmatism

Supporting Information:

- Text S1
- Figure S1
- Figure S2
- Table S1
- Supporting information 1

Correspondence to:

O. Forni,
olivier.forni@irap.omp.eu

Citation:

Forni, O., et al. (2015), First detection of fluorine on Mars: Implications for Gale Crater's geochemistry, *Geophys. Res. Lett.*, 42, 1020–1028, doi:10.1002/2014GL062742.

Received 4 DEC 2014

Accepted 24 JAN 2015

Accepted article online 29 JAN 2015

Published online 25 FEB 2015

First detection of fluorine on Mars: Implications for Gale Crater's geochemistry

Olivier Forni^{1,2}, Michael Gaft³, Michael J. Toplis^{1,2}, Samuel M. Clegg⁴, Sylvestre Maurice^{1,2}, Roger C. Wiens⁴, Nicolas Mangold⁵, Olivier Gasnault^{1,2}, Violaine Sautter⁶, Stéphane Le Mouélic⁵, Pierre-Yves Meslin^{1,2}, Marion Nachon⁵, Rhonda E. McInroy⁴, Ann M. Ollila⁷, Agnès Cousin⁴, John C. Bridges⁸, Nina L. Lanza⁴, and Melinda D. Dyar⁹

¹IRAP, UPS-OMP, Université de Toulouse, Toulouse, France, ²IRAP, CNRS, Toulouse CEDEX 4, France, ³Laser Distance Spectrometry, Petah Tikva, Israel, ⁴Los Alamos National Laboratory, Los Alamos, New Mexico, USA, ⁵Laboratoire de Planétologie et Géophysique de Nantes, Université de Nantes, Nantes, France, ⁶Muséum d'Histoire Naturelle, Paris, France, ⁷Chevron Energy Technology Company, Houston, Texas, USA, ⁸Space Research Centre, Department of Physics and Astronomy, University of Leicester, Leicester, UK, ⁹Department of Astronomy, Mount Holyoke College, South Hadley, Massachusetts, USA

Abstract Volatiles and especially halogens (F and Cl) have been recognized as important species in the genesis and melting of planetary magmas. Data from the Chemical Camera instrument on board the Mars Science Laboratory rover Curiosity now provide the first in situ analyses of fluorine at the surface of Mars. Two principal F-bearing mineral assemblages are identified. The first is associated with high aluminum and low calcium contents, in which the F-bearing phase is an aluminosilicate. It is found in conglomerates and may indicate petrologically evolved sources. This is the first time that such a petrologic environment is found on Mars. The second is represented by samples that have high calcium contents, in which the main F-bearing minerals are likely to be fluorapatites and/or fluorites. Fluorapatites are found in some sandstone and may be detrital, while fluorites are also found in the conglomerates, possibly indicating low-T alteration processes.

1. Introduction

Fundamental questions exist about the amount and the nature of volatiles in the Martian crust and mantle. Indeed, elements such as hydrogen and halogens may play a key role during partial melting of the mantle and in the alteration processes that can subsequently affect primary igneous rocks. On the basis of bulk compositions of SNC meteorites, it has been suggested that the Martian mantle is relatively rich in chlorine and fluorine and poor in water compared to the Earth [Dreibus and Wänke, 1985, 1987; Filiberto and Treiman, 2009a; Taylor et al., 2010]. A Cl-rich and H₂O-poor Martian mantle is feasible from the point of view of phase equilibria, and chlorine may play a role in Martian mafic magmas comparable to that of H₂O in terrestrial magmas [Filiberto and Treiman, 2009b]. A Cl-rich Martian mantle is consistent with nearly all observations including SNC meteorite compositions [Sautter et al., 2006], orbital Gamma Ray Spectrometer observations [Taylor et al., 2010], observations by the Spirit and Opportunity landers [Gellert et al., 2004; Rieder et al., 2006], and by the Phoenix lander [Hecht et al., 2009]. However, other studies have argued that the Martian mantle may have water contents comparable to that of the Earth [McSween et al., 2001; McCubbin et al., 2009; Stolper et al., 2013]. Indeed, the recently discovered ancient Martian meteorites Northwest Africa (NWA) 7034 [Agee et al., 2013] and NWA7533 [Humayun et al., 2014] have a much larger water content than the younger and drier shergottites. However, there is an increasing evidence that a large fraction of this water is not magmatic but located in secondary alteration phases like hydrous Fe-rich oxides and phyllosilicates [Muttik et al., 2014; Nemchin et al., 2014].

In contrast to the ubiquitous Cl observations, no fluorine has been reported so far on Mars. This is largely due to the inability of the instruments on Viking, Pathfinder, Spirit, and Opportunity to analyze fluorine. Within the SNC meteorites, magmatic inclusions commonly contain amphiboles and micas which can readily accept F up to a concentration of 3 wt % [Beck et al., 2006; Johnson et al., 1991]. Apatite is also a ubiquitous magmatic mineral in the SNC meteorites. It is a significant reservoir of halogens in the SNC meteorites and has been used to estimate the halogen budget of Mars [Patiño Douce et al., 2011].

We report here the first analyses of fluorine on Mars, using the Chemical Camera (ChemCam) [Maurice et al., 2012; Wiens et al., 2012] data at Gale Crater. This detection is made possible by the observation of CaF

molecular bands in the Laser-Induced Breakdown Spectroscopy (LIBS) spectra at remote distances [Gaft *et al.*, 2014]. They yield a much better F sensitivity than atomic emission lines, with an improved limit of detection (LoD) of ~0.2 wt % rather than several percent [Cremers and Radziemski, 1983].

2. Measuring Fluorine and Chlorine With ChemCam: Experiments

Halogens are difficult to detect with LIBS via their atomic or ionic emission lines. The difficulty of detecting halogens with LIBS is attributed to, among other factors, their energy level distribution. For example, the strongest emission lines for fluorine and chlorine are in the vacuum ultraviolet (VUV) spectral range at 95.5 and 134.7 nm for F and Cl, respectively. Detection capability in this region is limited by atmospheric absorption and laser coupling as well as by detector sensitivity. Other optical transitions exist in the 500–850 nm range but with relatively high LoD around 5 wt % [Cremers and Radziemski, 1983], which is not well suited for most geological studies. These are transitions between the excited states $(n + 1)s^4P - (n + 1)p^4D$ manifold ($n = 2$ for F and $n = 3$ for Cl), corresponding to wavelengths centered around 685.6 nm for F and 837.6 nm for Cl. Detection in this spectral region is more practical than in the VUV region, but these lines have upper levels of 10.40 and 14.50 eV, respectively, above the ground state [Cremers and Radziemski, 1983]. The detection limits for these lines are less than satisfactory for demanding applications. An alternative path to increase the LoD by an order of magnitude is to use molecular lines, which are formed when atoms recombine in the cooling plasma [Gaft *et al.*, 2014; Parigger, 2013]. However, molecular analysis by LIBS has been much less investigated than elemental LIBS. Most of the observed LIBS molecular emissions are oxides for which the ambient air typically supplies the O atom [Cremers and Radziemski, 2006]. For the halogens, a different combination is required, and the most easily observed is with Ca. In order to investigate this problem, LIBS experiments on fluorine- and chlorine-bearing samples have been performed [Gaft *et al.*, 2014] using various delay intervals between the laser and the spectral exposure to accurately describe the temporal evolution of the molecular emissions.

2.1. Fluorine-Bearing Materials

The initial experiments were performed on natural fluorite CaF_2 . The spectral features depend on the delay time applied to the spectral acquisition, and it is observed that with a delay time longer than 5.0 μs , the Ca atomic and ionic emission lines are quenched and only the molecular bands at 532.1, 584.5, 603.1 and 623.6 nm remain. Their relative intensities change somewhat as a function of the delay time: at 25 μs , the band at 602.9 nm is the strongest, while the other bands are relatively less intense. These bands are similar to those known from arc-induced plasma. The band centered at 532.1 nm is associated with the green $B2\Sigma - X2\Sigma$ systems, while the bands centered at 584.5, 603.1, and 623.6 nm are associated with the orange $A2\Pi - X2\Sigma$ systems of the diatomic CaF molecule. The band centered at 552.3 nm belongs to the green system of the CaO molecule [Peterson and Jaffe, 1953; Pearse and Gaydon, 1941].

The temporal evolution of a CaF_2 plasma plume was measured by the kinetic series method, which involves taking individual spectra at selectable time intervals using preset time-gating parameters. The emission of Ca II lines decay very rapidly, with a decay time of approximately 140 to 150 ns, while the emission of Ca I line decays slower, with a decay time of approximately 700 ns. The molecular emission of CaF is temporally broader compared to the ionic species. It reaches its maximum after approximately 800 ns followed by a decrease with a decay time of 4 to 6 μs . These behaviors correspond well to this kind of band, where in ablation plasma, it has a temporal plateau in the 400 to 600 ns interval [Oujja *et al.*, 2010]. Thus, such bands persist after a relatively long delay time of several microseconds, while ion emission lines are mostly quenched. The bands themselves are characterized by different plasma temporal evolution. The decay of the band at 532.8 nm may be approximated by two exponential laws with decay times of 1.1 and 4.5 μs ; at 583.0 nm, it is characterized by one exponential law with a decay time of 4.0 μs ; at 600.2 nm, it is by two exponential laws with decay times of 1.1 and 6.2 μs ; and at 622 nm, it is by one exponential law with decay time of 4.5 μs . The longest decay component of the band at 600.2 is 3 orders of magnitude longer than the radiative lifetime of vibronic levels of the $B2\Sigma - X2\Sigma$ states for different molecules, including CaF [Berg *et al.*, 1996]. Thus, the decay time is connected to the lifetime of those molecules in the plasma plume.

The band at 603.1 nm behaved differently from the other bands as a function of the laser energy. At lower excitation energy, all molecular CaF emission bands were stronger in comparison to calcium emission lines than at higher excitation energy, and the long-wavelength orange band at 603.1 nm became relatively

more intense than the others at low laser intensity. Differences between the orange system bands can be explained by the band at 603.1 nm belonging to the (0-0) transition, while the other bands belonged to (1-0) and (1-1) transitions.

To better understand the F molecular emissions, various F-bearing terrestrial analogues were analyzed starting with cryolite [Na₃AlF₆], which has the highest fluorine content of any common non-Ca-bearing mineral. This mineral did not exhibit such bands in its emission spectra. The same result was observed for calcite [CaCO₃], which is a calcium-bearing mineral without fluorine, whose emission spectra contain only Ca I emission lines and CaO emission bands, peaking at approximately 550 and 623 nm, respectively. Finally, a powder mixture of cryolite and calcite, containing both calcium and fluorine but not in the same constituents, exhibited CaF bands in its emission spectrum. Fluorine- and calcium-bearing minerals with lower fluorine content than fluorite [CaF₂] were studied, such as magmatic fluorapatite [Ca₅(PO₄)₃(F, OH)], sedimentary carbonate apatite (francolite) [Ca₅(PO₄CO₃)₃(F,OH)], apophyllite [KCa₄Si₈O₂₀F·8H₂O], and charoite [K(Ca,Na)₂Si₄O₁₀(OH,F)·H₂O]. The breakdown spectra of these minerals demonstrate that the detection sensitivities of CaF molecular emission bands, whose intensity is in proportion to the fluorine content, can be compared with that of the ionic F I emission line. Two other minerals were used: fluorite with approximately 50 wt % fluorine content and apophyllite with approximately 2 wt %. The strongest F I emission lines at 685.6 and 690.2 nm appeared in fluorite emission spectra with a minimal delay time of 100 ns. Apophyllite, with 25 times lower fluorine content than fluorite, did not exhibit F I emission lines. CaF bands were clearly visible not only in apophyllite but also in charoite with approximately 0.4 wt % fluorine content.

The above experiments were performed at ambient Earth pressure; some were also performed in vacuum. In order to better characterize and quantify the fluorine content through its molecular emissions, as part of this work, experiments have been conducted mixing fluorite with a certified basalt powder standard, BHVO-2, under Martian pressure conditions on the ChemCam-dedicated setup [Wiens *et al.*, 2013] at Los Alamos National Laboratory. Twelve mixing ratios ranging from 0.07 wt % to 50 wt % CaF₂ were analyzed, and for each of them, 5 observation points were acquired. The 30 spectra at each observation point were averaged together. After careful processing of the data [Wiens *et al.*, 2013], it is possible to draw a relationship between the area of the CaF emission band centered at 603 nm and the amount of fluorine present in the sample (Text S1 and Figure S1 in the supporting information). With these new calibration experiments, realistic for ChemCam, a detection limit of 0.2 wt % fluorine can be reached (Figure S1 in the supporting information).

2.2. Chlorine-Bearing Materials

Molecular emission of CaCl was studied using only CaCl₂, as minerals containing both Ca and Cl are relatively rare and were not at our disposal. Broad, long-lived emission bands were found in the orange part of the spectrum, with a peak at 593.5 corresponding to the CaCl orange system and peaks at 606.8, 618.8, and 631.4 nm belonging to the red system of CaCl. These emissions correspond to transitions from the B2Σ⁺ + A2Π levels to the X2Σ⁺ + ground level [Peterson and Jaffe, 1953; Pearse and Gaydon, 1941; Walters and Barrat, 1928]. The connection with the CaCl molecule was confirmed by the fact that calcium-bearing calcite (CaCO₃) and chlorine-bearing sylvite (KCl) do not contain such bands in their breakdown spectra, while a mixture of the two exhibits narrow bands centered at 592.9, 606.5, 617.6, 620.0, and 630.0 nm. Bands centered at 550 and 615 nm in the calcite breakdown spectra are connected to the green and orange emission bands of the CaO molecule [Peterson and Jaffe, 1953]. Those bands have a long lifetime of about 5 μs and appear in all calcium-bearing minerals. As with the fluorine, LIBS sensitivities of molecular CaCl and ionic Cl I can be compared. A weak line of Cl I peaking at 837.6 nm was detected in CaCl₂, whose chlorine content is approximately 64 wt %. It is not detected in a mixture of CaCO₃ with 10 wt % CaCl₂. Using molecular CaCl emission, Cl was detected not only in this sample but also in a mixture of CaCO₃ with 1.0 wt % of CaCl₂ corresponding to a concentration of 0.6 wt % Cl.

Finally, it must be stressed that because these are molecular emissions, the detectability of the halogens is dependent upon sufficient abundance of calcium. In other words, without calcium, halogens would not be detected by molecular emission lines even if present. In the case of targets with low calcium content and high halogen content, there may not be enough calcium atoms to recombine with the halogens, implying that the halogen contents will be underestimated. The interaction efficiency can also be reduced by elements substituting to Ca, like Sr, but generally, the amount of substituting element is low, and the effect is expected

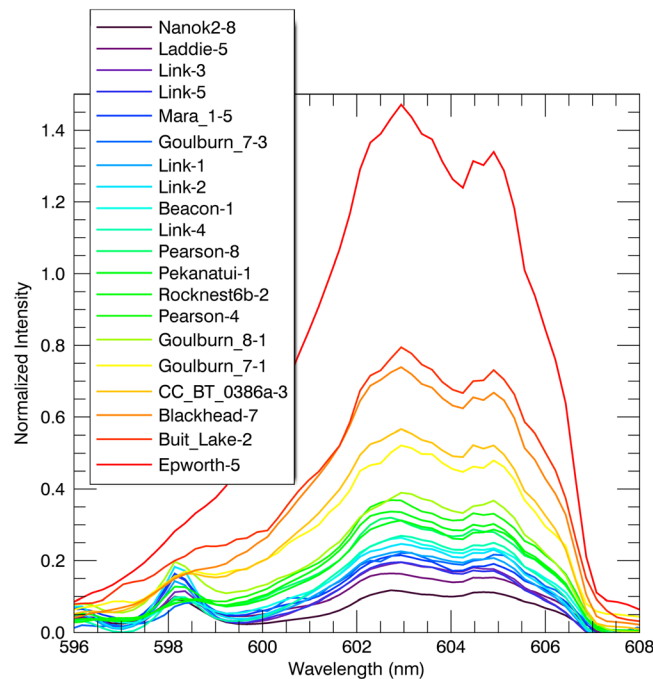


Figure 1. Spectral region between 596 nm and 608 nm of the rocks exhibiting the characteristic CaF molecular signature. The highest intensity corresponds to a fluorine content of about 5.5 wt % for Epworth #5 and the lowest to a fluorine content of about 0.6 wt %. The atomic line centered at 598.2 nm is a Si II emission line. The legend gives the names of the targets and the number of the ChemCam observation point on that target.

data on fluorite (CaF_2). The atomic lines of F I were also seen at 685.8, 687.2, 690.4, and 691.2 nm. In order to constrain the host minerals of the fluorine in that observation, we have studied how the concentrations of F vary with other mineral-forming elements on a shot to shot basis. Most elements were found to have a negative correlation with F, but calcium was a clear exception, showing a strong positive correlation. Strontium lines also showed this behavior, consistent with the fact that strontium is known to substitute for calcium in many minerals. Evidence for a positive correlation between fluorine and phosphorous was also found for this analysis point. Indeed, the strongest emission lines of P within the ChemCam observation range at 253.6, 256.4, and 256.6 nm have been observed (Figure S2 in the supporting information). This observation also indicates that P concentrations are high, given that the detection sensitivity of these particular lines is poor.

If the simultaneous variations of F, Ca, and P were those of a single mineral, we would conclude that it is fluorapatite [$\text{Ca}_5(\text{PO}_4)_3\text{F}$]. The latter stoichiometrically contains ~4 wt % F, 56 wt % CaO, and 42 wt % P_2O_5 . However, as mentioned earlier, the F content of Epworth #5 is $\sim 5.5 \pm 0.5$ wt %, and we have calculated a total amount of CaO of 24 ± 3 wt % using the partial least squares method [Wiens *et al.*, 2013]. Thus, there is too much F for fluorapatite only, and an additional F-rich mineral is required to explain the observations. Fluorite [CaF_2] is the most probable solution since the fraction of F in fluorite is 0.49, and 5.5 wt % fluorine would account for around 8.0 wt % CaO.

In addition to Epworth #5, strong CaF molecular bands have also been observed at Blackhead #7 (sol 367) and at the third point of a blind raster on sol 386 (CC_BT_0386a #3). Blackhead is a rough ventifacted textured rock with no grains and without apparent layering. CC_BT_0386a is a conglomerate. These points exhibit the phosphorous lines at 253.7 nm and/or 253.4 nm, making them similar to Epworth #5, indicating the presence of fluorapatite. In these two spectra, the F content is estimated to be $\sim 3.0 \pm 0.4$ wt %, which could correspond to pure fluorapatite. However, the CaO content of these two targets is ~ 17 wt %, which is too low for a pure fluorapatite. Consequently, here also, fluorite is probably part of the fluorine-bearing assemblage.

Following Epworth #5, Blackhead #7, and CC_BT_0386a #3, the conglomerates Goulburn (sol 19) and Link (sol 27) [Williams *et al.*, 2013] also show strong CaF signatures. It is of significant note that all the observation points

to be small. For example, in the case of the sample “Link” (see below), which is very Sr rich [Ollila *et al.*, 2014], the Sr content is nevertheless only about 1600 ppm, a concentration much lower than the total calcium available.

3. Measuring Fluorine and Chlorine With ChemCam: Observations

Among more than 2500 observation points that have been sampled by ChemCam over the first 400 days of the mission, more than 20 points in 13 rocks exhibiting a CaF molecular emission have been identified (Figure 1 and Table S1 in the supporting information). The strongest fluorine signature was observed on Martian solar day (sol) 72 on the fifth point of the Epworth soil target [Meslin *et al.*, 2013; Cousin *et al.*, 2015] in which a 1 mm diameter light-toned gravel lag was sampled with 30 laser shots. A preliminary estimate of the fluorine content yields $\sim 5.5 \pm 0.5$ wt % F based on the strength of the CaF emission from laboratory

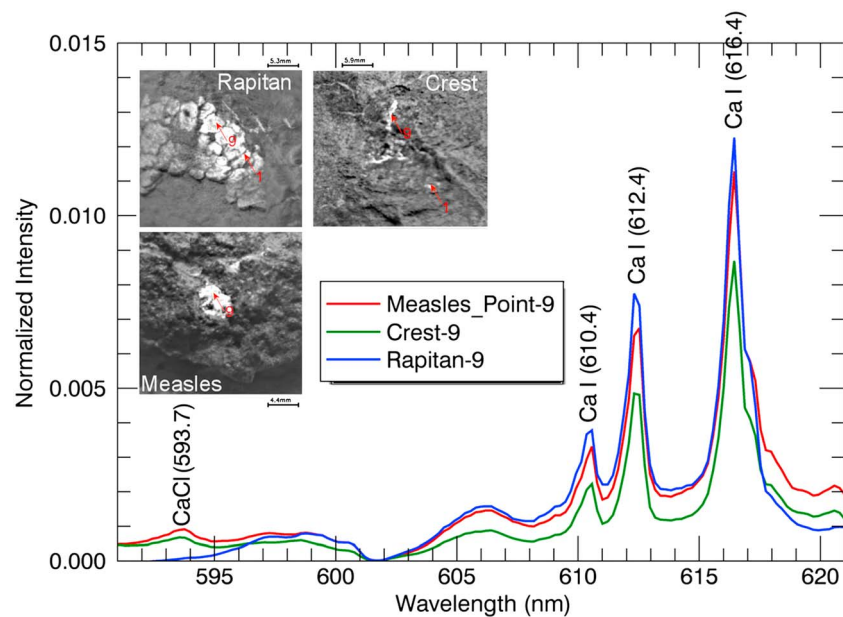


Figure 2. Spectra of the rocks showing the CaCl molecular emission at 594.6 nm, indicative of NaCl. The spectrum of a rock (Rapitan) having a similar composition but without chlorine is shown for comparison. All these observation points are calcium sulfate dominated and appear white on the images of ChemCam remote microimager.

in these conglomerates contain F, which is an indication that it is globally distributed and represents a bulk element in these rocks. Fluorine concentrations are estimated to be between 0.8 ± 0.2 and 2.4 ± 0.3 wt %, with Al_2O_3 content on the order of 18 ± 3.0 wt %. Unlike the three targets mentioned earlier, these rocks have low CaO contents, on the order of 5.0 wt%. Furthermore, a shot to shot analysis confirms that among all the major elements, silicon and aluminum are the elements that show the best positive correlations with the CaF signature followed by potassium and calcium. These correlations are confirmed by an Independent Component Analysis (ICA) algorithm [Hyvärinen *et al.*, 2001; Forni *et al.*, 2013]. One of the ICA components is characterized by the CaF signature along with contributions from Al. In terms of the mineral host of F, we also note that the K_2O content is relatively high, on the order of 2.5 wt %, with a high K/Na ratio and that the hydrogen signature, at least for Link, is noticeable [Williams *et al.*, 2013]. This enrichment in K is also supported by the observed trace elements and particularly by the high rubidium and barium abundances found in Link [Ollila *et al.*, 2014]. Phlogopite [$\text{KMg}_3\text{AlSi}_3\text{O}_{10}(\text{F},\text{OH})_2$] is considered an unlikely host for F in light of the low MgO content (~ 1 wt %) of these analyses, the low Fe and Mg contents also arguing against amphiboles. On the other hand, muscovite [$\text{KAl}_2[\text{AlSi}_3\text{O}_{10}](\text{OH},\text{F})_2$] and topaz [$\text{Al}_2[\text{SiO}_4](\text{OH},\text{F})_2$] are considered as plausible candidates especially points #2 and #4 of Link that show a nice correlation with Si, Al, and K (Table S1 in the supporting information). However, topaz and muscovite have SiO_2 contents around 33 wt % and 48 wt %, respectively, much lower than the abundances we observe in the conglomerates. Keeping in mind that we generally observe mixtures of minerals within the ~ 0.4 mm diameter beam [Maurice *et al.*, 2012], topaz and/or muscovite could be mixed with a phase richer in silica, such as alkali feldspar [Sautter *et al.*, 2014], that could also be contributing alkalis and certain trace elements. However, fluorite cannot be discounted as the sole fluorine-bearing phase, especially in points #1 and #3, but apatite can because of the low bulk Ca contents.

Additional F-bearing observation points have been found periodically along the rover traverse (Table S1 in the supporting information). All these points generally have higher calcium and lower aluminum compared to the conglomerates described earlier. These are all likely to be fluorapatite, even if the phosphorous lines are not visible, since F is correlated with calcium in a shot to shot analysis. However, fluorite cannot be discounted as the F-bearing phase. This is the case for the targets belonging to the Rocknest unit (Pearson and Rocknest6b) and for two targets (Nanok and Laddie) that are very similar to those observed in the Rocknest unit [Blaney *et al.*, 2014]. However, a fraction of the rocks displaying the fluorine signature is also iron rich and often enriched in alkalis, especially potassium. The presence of these elements is consistent with

a number of possible F-bearing minerals, including biotite or amphiboles. This is the case for observations that are found in porphyritic igneous rocks [Sautter *et al.*, 2014] (Mara1 #5 and Beacon #1; Table S1 in the supporting information), in which the fluorine content is estimated to be about 1.2 ± 0.3 wt %.

Chlorine is also detected via CaCl molecular bands. Crest #9 (sol 125) and Measles #9 (sol 305) show evidence for chlorine (Figure 2). These samples are characterized by high calcium concentrations, and their spectra display sulphur lines [Nachon *et al.*, 2014]. Surprisingly, no other sulphur-rich targets among the many sulphate veins observed in Yellowknife Bay [Grotzinger *et al.*, 2013] exhibit the CaCl band. These two observations are unique in having relatively high sodium concentrations, suggesting NaCl as a possible phase for chlorine, recombining with calcium in the plasma.

In summary, we can confidently show that none of the fluorine-bearing observations with or without phosphorous show the presence of chlorine, at least above the 0.6 wt % detection limit [Gaft *et al.*, 2014], although this value has to be refined with experiments under Martian atmospheric conditions.

4. Discussion

The F-bearing parageneses found in the Gale conglomerates [Williams *et al.*, 2013] are very peculiar, and with their silica-, aluminum-, and alkali-rich compositions, they appear to be unique to the Mars Science Laboratory (MSL) landing site. These mineralogies are moreover very distinct to those found in the SNC meteorites.

The observed enrichments in K and Al (and Rb and Ba in the case of Link [Ollila *et al.*, 2014]) suggest the presence of an alkali feldspar under the laser beam, consistent with phase equilibria at low temperature in the system $K_2O-Na_2O-Al_2O_3-SiO_2-F_2O_{-1}-H_2O$ [Manning, 1981; Dolejs and Baker, 2007]. In terms of F-bearing phases in this system, it has been shown that at 100 MPa, near-solidus melts may saturate with topaz or cryolite, but the associated melt will contain low fluorine concentrations if the activity of alumina is buffered by micas or aluminosilicates in the crystallizing assemblage [Dolejs and Baker, 2007]. On the other hand, if only quartz and feldspars are crystallizing from residual melts, either topaz or cryolite will eventually crystallize, but the melt will continue its enrichment in fluorine. However, saturation in Al-rich F-bearing minerals requires low concentrations in CaO, as fluorite saturation typically occurs before that of Al-rich phases. Indeed, natural and experimental peralkaline (alkali-rich) and met-aluminous magmas saturate in fluorite, buffering fluorine concentrations in the liquids to low levels, on the order of 0.5–1 wt % F [Scaillet and MacDonald, 2004; Dolejs and Baker, 2006]. Fluorite saturation may also occur in F-rich peraluminous (Al-rich) melts, but very high CaO concentrations are required in this case; thus, magmatic crystallization of fluorite in topaz-bearing silicic suites is suppressed.

The relatively high observed fluorine contents are thus consistent with the presence of topaz and/or muscovite (Table S1 in the supporting information). Alternatively, if fluorite is the F host in the conglomerates, this would be difficult to reconcile with a peraluminous magmatic system, as discussed above, although its presence may result from a secondary hydrothermal process as described in many pegmatitic systems, implying temperatures on the order of 500°C, possibly associated with impact cratering. Alternatively, it has been proposed that fluorite can form in secondary alteration systems [Filiberto and Schwenzer, 2013] especially at low temperature and low water/rock ratios. Although the protolith at Gale Crater may be more feldspathic than the Home Plate formation at Gusev [Sautter *et al.*, 2014], the simulations of Filiberto and Schwenzer [2013] indicate that the formation of fluorite is thermodynamically stable and produced in significant amount, a prediction which nicely fits our observations. However, in these same conditions and in presence of CO_2 , carbonates are a major output phase of the simulation but not observed so far in Gale Crater.

In addition to Epworth #5, Blackhead #7, and CC_BT_0386a #3, the following targets have lower but still clear coenrichments of F and Ca (Pekantui, Pearson, Rocknest6, Laddie, Nanok2, and Buit_Lake; Table S1 in the supporting information) and are thus probably dominated by a contribution from apatite. When apatite within the SNC meteorites is compared to apatite from terrestrial basalts, it is found that the Martian phosphates are poorer in water. In detail, Chassigny and Nakhilite meteorites contain two populations of apatite: fluorine-rich and water-poor population, found in melt inclusions, and chlorine-rich and water-poor population, found interstitially [McCubbin *et al.*, 2008, 2013]. These observations are interpreted in terms of a high-temperature closed-system process that forms fluorapatite within melt inclusions and a lower temperature

open-system process that forms interstitial chlorapatite associated with fluid migration [McCubbin *et al.*, 2013]. Indeed, experimental data have demonstrated that metasomatic apatites tend to be Cl rich, while magmatic apatites tend to be F rich [Patiño Douce *et al.*, 2011]. However, the Cl-rich apatites observed in the Nakhilites and Chassignites do not necessarily imply external fluids, as Cl-rich fluids may be directly related to late-stage magmatism, relaxing many of the previous constraints used to rule out the Nakhilites and Chassignites as comagmatic rocks [McCubbin *et al.*, 2013]. The situation at Gale is clearly different, since chlorine at the LoD of 0.6 wt % is never detected in F-bearing samples, indicating that the apatites observed by ChemCam, if primary, did not experience this interaction with comagmatic Cl-rich fluids. Furthermore, the existence of F-rich apatite measured at the surface of Mars may call into question the idea that the Martian mantle is Cl rich [Filiberto and Treiman, 2009b], arguing instead for an important role of fluorine. Our data therefore support the recent idea that fluorine is a key element affecting the petrogenesis of Martian basalts, since fluorine also has a large effect on liquidus depression of basalts and the chemistry of crystallizing minerals [Filiberto *et al.*, 2012]. These effects will be especially important for low-degree partial melts, which may start with relatively high abundances of fluorine and produce silica-poor and alkali-rich magmas. It is also of note that apatites occur in many hydrothermal systems on Earth. The famous Durango apatite is of hydrothermal origin, occurring in the Tertiary hydrothermally related iron-magnetite deposits of the Cerro de Mercado deposit of Mexico [Piccoli and Candela, 2002]. This setting may be somewhat similar to the Rocknest unit that is characterized by low silicon content and high iron and titanium, reflecting the probable presence of ferrous and/or titaniferrous oxides like magnetite, hematite, and/or ilmenite. In this hydrothermal context, apatites may also be enriched in sulphur [Piccoli and Candela, 2002], whose presence is indeed suggested in the Rocknest unit. The few targets belonging to the Gillespie Lake sandstones [Mangold *et al.*, 2015], part of the Yellowknife Bay unit, are unlikely to have formed in situ by hydrothermal alteration, given the low grade of local diagenetic alteration [McLennan *et al.*, 2014]. Moreover, apatites that form in a diagenetic context are, on Earth, related to organic matter and biologic activity [Krom and Berner, 1981; Knudsen and Gunter, 2002], a process unlikely on Mars. They are also often accompanied by the presence of francolite [$\text{Ca}_5(\text{PO}_4)_3(\text{F},\text{OH})$] [McArthur, 1985], which has not been observed in Gale Crater. Apatite at Yellowknife Bay may thus correspond to detrital grains deposited by past rivers, not enabling us to discuss their initial formation as magmatic or hydrothermal, despite the fact that many apatites found in the mesostasis of the nakhilites, likely to be hydrothermal, contain a large amount of chlorine [Bridges and Schwenzer, 2012].

These new analyses point to an important role of F on Mars. First of all, the presence of multiple primary F-bearing minerals in rocks that are likely related to magmatism around the crater rim of Gale may have important implications for petrogenesis during mantle melting. Second, the unique environment represented by the conglomerates found in the early days of the mission (Table S1 in the supporting information) implies a high degree of differentiation of primary magmas at Gale Crater, similar to that found in granodioritic settings. The large amount of alkali feldspar and plagioclase combined with the observation of quartz normative mineralogy [Sautter *et al.*, 2014] supports this interpretation, and it is of interest to consider to what extent halogens play a role in this process. Finally, the large amount of secondary F-bearing phases, like fluorapatites and fluorite, can put stringent constraints on the fluid composition, temperature, and pH conditions that led to the alteration of the primary rocks.

Acknowledgments

The development and operation of the ChemCam instrument was supported in France by funds from the French space agency, Centre National d'Etudes Spatiales. Support was also received from INSU/CNRS. Support for the development and operation in the U.S. was provided by NASA to the Mars Exploration Program and specifically to the MSL team. Imaging and chemical data presented here are available in the NASA Planetary Data System <http://pds-geosciences.wustl.edu/missions/msl>. We are grateful to the MSL engineering and management teams (and especially the Jet Propulsion Laboratory, California Institute of Technology, under contract with NASA) for making the mission and this scientific investigation possible and to science team members who contributed to mission operations. We thank Pamela Conrad and an anonymous reviewer for their constructive remarks that greatly improved the manuscript.

The Editor thanks two anonymous reviewers for their assistance in evaluating this paper.

References

- Agee, C. B., *et al.* (2013), Unique meteorite from early Amazonian Mars: Water-rich basaltic breccia Northwest Africa 7034, *Science*, 339, 780–785.
- Beck, P., J.-A. Barrat, P. Gillet, M. Wadhwa, I. A. Franchi, R. C. Greenwood, M. Bohn, J. Cotten, B. V. de Moorlele, and B. Reynard (2006), Petrography and geochemistry of the chassignite Northwest Africa 2737 (NWA 2737), *Geochim. Cosmochim. Acta*, 70, 2127–2139.
- Berg, L., K. Ekvall, and S. Kelly (1996), Radiative lifetime measurements of vibronic levels of the $\text{B}2\Sigma^+$ state of CaH by laser excitation spectroscopy, *Chem. Phys. Lett.*, 257, 351–355.
- Blaney, D., *et al.* (2014), Chemistry and texture of the rocks at Rocknest, Gale Crater: Evidence for sedimentary origin and diagenetic alteration, *J. Geophys. Res. Planets*, 119, 2109–2131, doi:10.1002/2013JE004590.
- Bridges, J. C., and P. S. Schwenzer (2012), The nakhilite hydrothermal brine on Mars, *Earth Planet. Sci. Lett.*, 359–360, 117–123.
- Cousin, A., *et al.* (2015), Compositions of coarse and fine particles in Martian soils at Gale: A window into the production of soils, *Icarus*, 249, 22–42, doi:10.1016/j.icarus.2014.04.052.
- Cremers, D., and L. Radziemski (1983), Detection of chlorine and fluorine in air by Laser-Induced Breakdown Spectrometry, *Anal. Chem.*, 55, 1252–1256.
- Cremers, D., and L. Radziemski (2006), *Handbook of Laser-Induced Breakdown Spectroscopy*, Wiley, New York.
- Dolejs, D., and D. R. Baker (2006), Fluorite solubility in hydrous haplogranitic melts at 100 MPa, *Chem. Geol.*, 225, 40–60.

- Dolejs, D., and D. R. Baker (2007), Liquidus equilibria in the system $K_2O-Na_2O-Al_2O_3-SiO_2-F_2O_{-1}-H_2O$ to 100 MPa: I. Silicate-fluoride liquid immiscibility in anhydrous systems, *J. Petrol.*, *48*(4), 785–806.
- Dreibus, G., and H. Wänke (1985), Mars, a volatile-rich planet, *Meteoritics*, *20*(2), 367–381.
- Dreibus, G., and H. Wänke (1987), Volatiles on Earth and Mars: A comparison, *Icarus*, *71*(2), 225–240.
- Filiberto, J., and A. H. Treiman (2009a), Martian magmas contained abundant chlorine, but little water, *Geology*, *37*(12), 1087–1090.
- Filiberto, J., and A. H. Treiman (2009b), The effect of chlorine on the liquidus of basalt: First results and implications for basalt genesis on Mars and Earth, *Chem. Geol.*, *263*(1–4), 60–68.
- Filiberto, J., and S. P. Schwenzer (2013), Alteration mineralogy of Home Plate and Columbia Hills formation conditions in context to impact, volcanism, and fluvial activity, *Meteoritics Planet. Sci.*, *48*(10), 1937–1957.
- Filiberto, J., J. Wood, R. Dasgupta, N. Shimizu, L. Le, and A. H. Treiman (2012), Effect of fluorine on near-liquidus phase equilibria of an Fe-Mg rich basalt, *Chem. Geol.*, *312–313*, 118–126.
- Forni, O., S. Maurice, O. Gasnault, R. C. Wiens, A. Cousin, S. M. Clegg, J.-B. Sirven, and J. Lasue (2013), Independent component analysis classification of Laser-Induced Breakdown Spectroscopy spectra, *Spectrochim. Acta B*, *86*, 31–41.
- Gaft, M., L. Nagli, N. Eliezer, Y. Groisman, and O. Forni (2014), Elemental analysis of halogens using molecular emission by Laser-Induced Breakdown Spectroscopy in air, *Spectrochim. Acta, Part B*, *98*, 39–47.
- Gellert, R., et al. (2004), Chemistry of rocks and soils in Gusev Crater from the Alpha Particle X-ray Spectrometer, *Science*, *305*, 829–832.
- Grotzinger, J. P., et al. (2013), A habitable fluvio-lacustrine environment at Yellowknife Bay, Gale Crater, Mars, *Science*, doi:10.1126/science.1242777.
- Hecht, M. H., et al. (2009), Detection of perchlorate and the soluble chemistry of Martian soil at the Phoenix lander site, *Science*, *325*, 64–67.
- Humayun, M., et al. (2014), Origin and age of the earliest Martian crust from meteorite NWA7533, *Nature*, *503*, 513–516.
- Hyvärinen, J., J. Karhunen, and E. Oja (2001), *Independent Component Analysis*, Wiley, New York.
- Johnson, M. C., M. J. Rutherford, and P. C. Hess (1991), Chassigny petrogenesis—Melt compositions, intensive parameters, and water contents of Martian (questionable) magmas, *Geochim. Cosmochim. Acta*, *55*, 349–366.
- Knudsen, C. A., and M. E. Gunter (2002), Sedimentary phosphorites—An example: Phosphoria formation, Southeastern Idaho, U.S.A, in *Phosphates: Geochemical, Geobiological, and Materials Importance*, edited by M. J. Kohn, J. Rakovan, and J. M. Hughes, pp. 363–389, Min. Soc. Am., Washington, D. C.
- Krom, M. D., and R. A. Berner (1981), The diagenesis of phosphorous in a near-shore marine sediment, *Geochim. Cosmochim. Acta*, *45*, 207–216.
- Mangold, N., et al. (2015), Chemical variations in Yellowknife Bay formation sedimentary rocks analyzed by ChemCam onboard the Curiosity rover on Mars, *J. Geophys. Res. Planets*, doi:10.1002/2014JE004681.
- Manning, D. A. C. (1981), The effect of fluorine on liquidus phase relationships in the system Qz-Ab-Or with excess water at 1 kb, *Contrib. Mineral. Petrol.*, *76*(2), 206–215.
- Maurice, S., et al. (2012), The ChemCam instrument suite on the Mars Science Laboratory (MSL) rover: Science objectives and mast unit description, *Space Sci. Rev.*, *170*, 95–166.
- McArthur, J. M. (1985), Francolite geochemistry-compositional controls during formation, diagenesis, metamorphism and weathering, *Geochim. Cosmochim. Acta*, *49*, 23–35.
- McCubbin F. M., H. Nekvasil, A. D. Harrington, S. M. Elardo, and D. H. Lindsley (2008), Compositional diversity and stratification of the Martian crust: Inferences from crystallization experiments on the microbasalt Humphrey from Gusev Crater, Mars, *J. Geophys. Res.* *113*, E11013, doi:10.1029/2008JE003165.
- McCubbin, F. M., A. Smirnov, H. Nekvasil, J. Wang, E. H. Hauri, and D. H. Lindsley (2009), Hydrous magmatism on Mars: A source for water on the ancient Martian surface and current Martian subsurface?, *Lunar Planet. Sci.*, *XL*, 2207.
- McCubbin, F. M., S. M. Elardo, C. K. Shearer Jr., A. Smirnov, E. H. Hauri, and D. S. Draper (2013), A petrogenetic model for the comagmatic origin of chassignites and nakhlites: Inferences from chlorine-rich minerals, petrology, and geochemistry, *Meteorit. Planet. Sci.*, *48*, 819–853.
- McLennan, S. M., et al. (2014), Elemental geochemistry of sedimentary rocks at Yellowknife Bay, Gale Crater, Mars, *Science*, *343*, doi:10.1126/science.1244734.
- McSween, H. Y., T. L. Grove, R. C. F. Lentz, J. C. Dann, A. H. Holzheid, L. R. Riciputi, and J. G. Ryan (2001), Geochemical evidence for magmatic water within Mars from pyroxenes in the Shergotty meteorite, *Nature*, *409*, 487–490.
- Meslin, P.-Y., et al. (2013), Soil diversity and hydration as observed by ChemCam at Gale Crater, Mars, *Science*, *341*, doi:10.1126/science.1238670.
- Muttik, N., F. M. McCubbin, L. P. Keller, A. R. Santos, W. A. McCutcheon, P. P. Provencio, Z. Rahman, C. K. Shearer, J. W. Boyce, and C. B. Agee (2014), Inventory of H_2O in the ancient Martian regolith from Northwest Africa 7034: The important role of Fe oxides, *Geophys. Res. Lett.*, *41*, 8235–8244, doi:10.1002/2014GL062533.
- Nachon, M., et al. (2014), Calcium sulfate veins characterized by the ChemCam instrument at Gale Crater, Mars, *J. Geophys. Res. Planets*, *119*, 1991–2016, doi:10.1002/2013JE004588.
- Nemchin, A. A., M. Humayun, M. J. Whitehouse, R. H. Hewins, J. P. Lorand, A. Kennedy, M. Grange, B. Zanda, C. Fieni, and D. Delicque (2014), Record of the ancient Martian hydrosphere and atmosphere preserved in zircon from a Martian meteorite, *Nat. Geosci.*, *7*(9), 638–642.
- Ollila, A. M., et al. (2014), Trace element geochemistry (Li, Ba, Sr, and Rb) using Curiosity's ChemCam: Early results for Gale Crater from Bradbury landing site to Rocknest, *J. Geophys. Res. Planets*, *119*, 255–285, doi:10.1002/2013JE004517.
- Oujia, M., R. de Nalda, M. Lopez-Arias, R. Torres, J. Morangos, and M. Castillejo (2010), CaF_2 ablation plumes as a source of CaF molecules for harmonic generation, *Phys. Rev. A*, *81*, 04384-1-04384-7.
- Parigger, C. (2013), Atomic and molecular emissions in Laser-Induced Breakdown Spectroscopy, *Spectrochim. Acta, Part B*, *79–80*, 4–16.
- Patiño Douce, A. E., M. F. Roden, J. Chaumba, C. Fleisher, and G. Yagodinski (2011), Compositional variability of terrestrial mantle apatites, thermodynamic modeling of apatite volatile contents, and the halogen and water budgets of planetary mantles, *Chem. Geol.*, *288*(1–2), 14–31.
- Pearse, R., and A. Gaydon (1941), *The Identification of the Molecular Spectra*, Wiley, New York.
- Peterson M., and H. Jaffe (1953), Visual arc spectroscopic detection analysis, *US Dept. of the Interior, Bur. Mines Bull.*, *524*.
- Piccoli M. P., and P. A. Candela (2002), Apatite in igneous systems, in *Phosphates: Geochemical, Geobiological, and Material Importance*, edited by M. J. Kohn, J. Rakovan, and J. M. Hughes, pp. 255–292, Min. Soc. Am., Washington, D. C.
- Rieder, R., et al. (2006), Chemistry of rocks and soils at Meridiani Planum from the Alpha Particle X-ray Spectrometer, *Science*, *306*, 1746.
- Sautter, V., A. Jambon, and O. Boudouma (2006), Cl-amphibole in the nakhlite MIL 03346: Evidence for sediment contamination in a Martian meteorite, *Earth Planet. Sci. Lett.*, *252*, 45–55.

- Sautter, V., et al. (2014), Igneous mineralogy at Bradbury Rise: The first ChemCam campaign at Gale Crater, *J. Geophys. Res. Planets*, *119*, 1–17, doi:10.1002/2013JE004472.
- Scaillet, B., and R. MacDonald (2004), Fluorite stability in silicic magmas, *Contrib. Mineral. Petrol.*, *147*(3), 319–329.
- Stolper, E. M., et al. (2013), The petrochemistry of Jake_M: A Martian mugearite, *Science*, *341*, doi:10.1126/science.1239463.
- Taylor, G. J., W. V. Boynton, S. M. McLennan, and L. M. V. Martel (2010), K and Cl concentrations on the Martian surface determined by the Mars Odyssey gamma ray spectrometer: Implications for bulk halogen abundances in Mars, *Geophys. Res. Lett.*, *37*, L12204, doi:10.1029/2010GL043528.
- Walters, O., and S. Barrat (1928), The alkaline Earth halide spectra and their origin, *Proc. R. Soc. London, Ser. A*, 118–120.
- Wiens, R. C., et al. (2012), The ChemCam instrument suite on the Mars Science Laboratory (MSL) Rover: Body unit and combined system tests, *Space Sci. Rev.*, *170*, 167–227.
- Wiens, R. C., et al. (2013), Pre-flight calibration and initial data processing for the ChemCam Laser-Induced Breakdown Spectroscopy instrument on the Mars Science Laboratory rover, *Spectrochim. Acta, Part B*, *82*, 1–12.
- Williams, R. M. E., et al. (2013), Martian fluvial conglomerates at Gale Crater, *Science*, *340*, 1068–1073.